

## Decomposition Pressures and Standard Enthalpy of Formation for the Iron Selenides FeSe, Fe<sub>7</sub>Se<sub>8</sub>, Fe<sub>3</sub>Se<sub>4</sub> and FeSe<sub>2</sub>

SVEN R. SVENDSEN

*Department of Chemistry, University of Oslo, Blindern, Oslo 3, Norway*

Vapour pressures of iron selenides in the composition range from FeSe<sub>3.88</sub> to FeSe<sub>0.96</sub> have been measured partly by means of Knudsen cells and partly by means of silica spiral gauge. The standard enthalpy of formation at 298 K for FeSe, FeSe<sub>1.143</sub>, FeSe<sub>1.333</sub>, and FeSe<sub>2</sub> has been determined to  $-17.7 \pm 1.4$  kcal/mol,  $-18.3 \pm 1.5$  kcal/mol,  $-20.5 \pm 2.1$  kcal/mol, and  $-29.4 \pm 2.9$  kcal/mol, respectively.

The iron-selenium system has been previously studied by several investigators<sup>1-13</sup> by means of X-ray, magnetic, electric, thermal, and metallographic methods. These investigations have shown that there exist at room temperature three intermediate phases: (1) The tetragonal PbO-like structure with the approximate composition Fe<sub>1.04</sub>Se (FeSe<sub>0.96</sub>). This is a phase with surplus iron atoms in interstitial positions. (2) The NiAs-like phase, which extends over a certain composition range at room temperature, at least from 53.3 to 57.1 at. % selenium. Within this range the phase exists as a hexagonal NiAs-like structure with approximate composition Fe<sub>7</sub>Se<sub>8</sub>, and as what can be considered a monoclinic deformation of the same phase, with approximate composition Fe<sub>3</sub>Se<sub>4</sub>. The phases should be written Fe<sub>1-x</sub>Se, because they are structures with iron vacancies when the selenium content increases. (3) The last and the most selenium-rich phase is iron diselenide with marcasite-like structure.

At temperatures high enough, the only solid phase that exists beside iron is that with the NiAs-like structure. The tetragonal phase undergoes a peritectoid reaction with the formation of the NiAs-like phase and iron at 458°C,<sup>13</sup> the monoclinic Fe<sub>3</sub>Se<sub>4</sub> goes through a λ-type transition with maximum at 704°C<sup>13</sup> (725°C this work) into the hexagonal structure, and FeSe<sub>2</sub> melts incongruently at 585°C forming the NiAs-like phase and a selenium-rich liquid. The NiAs-like phase melts congruently at *ca.* 1065°C with 53.6 at. % selenium. In the selenium-rich part of the system a monotectic exists at *ca.* 793°C. The

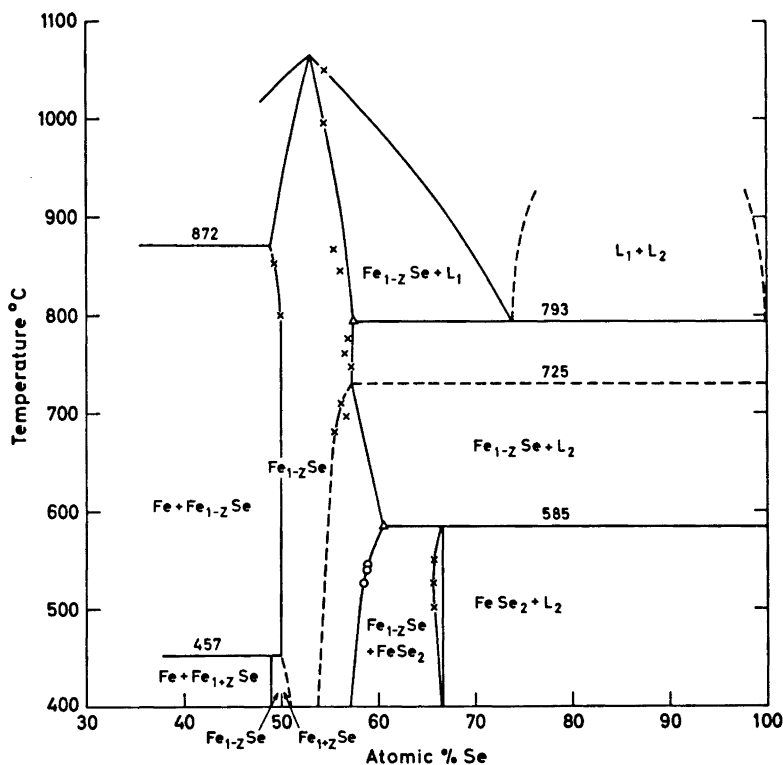


Fig. 1. Part of the iron-selenium phase diagram.  $\Delta$ , determined by micro-probe; O, from X-ray;  $\times$ , from vapour pressure.

two-liquid region extends from 73.9 to 99.98 at. % selenium<sup>10</sup> with a consolute temperature of *ca.* 1070°C at approximately 93 at. % selenium.

Fig. 1 shows part of the iron-selenium phase diagram which has direct relation to the present study. The construction is based partly on the literature cited, and partly on the present work.

#### EXPERIMENTAL

The decomposition pressures of the selenides in the composition range from FeSe<sub>3.88</sub> to FeSe<sub>1.15</sub> have been detected by a silica spiral gauge which acted as a null instrument, the actual pressures being measured with a conventional mercury filled U-tube. The apparatus has been described by Haraldsen *et al.*<sup>14</sup>

The dissociation pressures in the composition range from FeSe<sub>1.14</sub> to FeSe<sub>0.95</sub> were measured by means of Knudsen silica effusion cells. The cells of diameter and height 1.0 cm consist of two cylindrical halves ground to a close fit. The average diameter of the orifices was determined with a microscope equipped with a calibrated millimeter scale. Since the holes were not absolutely round, several measurements were made at evenly spaced diameters for the orifices. The maximum variation in the diameters was 2.1 %.

During effusion the cells were placed in a horizontal silica tube, contained in a furnace. The silica tube was connected to vacuum pumps. The system was evacuated and the furnace was brought up to the desired temperature before being positioned around the silica tube. 5–10 min elapsed before the furnace regained the set-point temperature. Vacuum was maintained by a silicone-oil diffusion pump with a liquid nitrogen cold trap, backed by a mechanical pump. A Penning gauge was used to measure the pressure, which was always maintained below  $5 \times 10^{-6}$  torr.

The cell temperature was measured by a calibrated Pt/Pt-10 % Rh thermocouple placed in a pocket close to the cell in the silica tube. Tests with the thermocouple located in exactly the same place as the cell showed that the temperature of the sample under study could be measured within  $\pm 1.0^\circ\text{C}$ . During an effusion run the temperature was kept within  $\pm 0.5^\circ\text{C}$  by means of a Leeds and Northrup temperature controller.

The weight loss of the cells was determined at room temperature by means of a micro balance.

*Materials.* Iron in the form of 5 mm rods (purity 4N8) was obtained from Koch-Light Laboratories, England. The selenium (purity 4N8), supplied by Boliden Gruvaktiebolag, Sweden, was twice vacuum sublimated.

*Preparations.*  $\text{FeSe}_{0.96}$ ,  $\text{FeSe}_{1.143}$ , and  $\text{FeSe}_{1.333}$  were prepared by heating accurately weighed quantities of iron rod and selenium in evacuated and sealed silica tubes. As a precaution against cracking, the charges with the two first mentioned compositions were sealed in double ampoules. The temperature was maintained at  $1000^\circ\text{C}$  for 4 weeks and then slowly lowered to room temperature over a period of one week. No free selenium could be detected in the tubes at the termination of the reaction period.

Two samples of  $\text{FeSe}_2$  were prepared from stoichiometric quantities of  $\text{FeSe}_{1.333}$  and selenium. The first sample was kept at  $340^\circ\text{C}$  for 6 months. The presence of unreacted selenium at the end of this period together with the analysis of the product (composition  $\text{FeSe}_{1.936}$ ) showed that the reaction was incomplete. The second sample was kept at  $520^\circ\text{C}$  but only for 6 weeks, and then slowly cooled to room temperature. This time less free selenium was found in the tube, and the analysis gave the composition  $\text{FeSe}_{1.973}$ .

X-Ray photographs of the prepared samples of the diselenides, taken with a Guinier camera, showed no other lines than the ones belonging to the orthorhombic phase. A small contamination of the specimens by lower iron selenides could be detected, however, by applying a magnet to the bulk material, because of the ferrimagnetism of the lower selenides. The diselenide itself is diamagnetic, as has been verified by neutron diffraction.<sup>15</sup>

*Chemical analysis.*  $\text{FeSe}_{1.333}$  and the two samples of  $\text{FeSe}_2$  prepared at different temperatures were analysed gravimetrically.

Samples were dissolved in concentrated  $\text{HNO}_3$  and the excess nitric acid expelled by heating with concentrated  $\text{H}_2\text{SO}_4$ . The solutions were diluted to 250 ml. Fifty ml portions were pipetted out and treated with hydrazine sulphate in order to reduce and precipitate the selenium. After digestion on a water bath, the selenium was filtered off in sintered glass crucibles, dried at  $105^\circ\text{C}$  for 1 h, cooled in a desiccator for 2 h and weighed. The iron contained in the filtrate was oxidized, precipitated as hydrous ferric oxide with ammonia, and ignited at  $1000^\circ\text{C}$  to constant weight. The results are presented in Table 1.

Table 1. Results of the gravimetric analysis.

Substance	Se/Fe ratio found			Formula
$\text{FeSe}_{1.333}$	1.324	1.324	1.330	$\text{FeSe}_{1.326}$
$\text{FeSe}_2$ (I)	1.938	1.936	1.934	$\text{FeSe}_{1.936}$
$\text{FeSe}_2$ (II)	1.972	1.970	1.977	$\text{FeSe}_{1.973}$

### Vapour pressure measurements with the spiral gauge

Static pressure measurements are particularly subject to errors from even minute amounts of easily volatilized impurities. In the samples studied, oxygen is the most likely contaminant, and the formation of gaseous  $\text{SeO}_2$  at higher temperatures cannot be excluded.

At high pressures the principal sources of error in the measurements were due to such volatilized impurities. In addition, at low pressures the errors in the null readings on the scale and the zero-point shifts became evident. The error in the reproducibility of the zero point setting is estimated to  $\pm 1$  torr.

The actual pressures were measured with a mercury-filled U-tube, 13 mm bore. The difference between the levels in the two limbs was read with a cathetometer to an accuracy of 0.01 mm. The overall error in the pressure data is difficult to estimate on account of the impurity tension. Only uncertainties due to reproducibility of zero-point on the scale can be given.

Except for  $\text{FeSe}_2$ , a comparatively short time was required to obtain equilibrium in the different composition ranges, both for increasing and decreasing temperatures.

Three experimental runs were performed. The first had as starting material 1.6355 g of  $\text{FeSe}_{1.333}$ , the second 2.9984 g of  $\text{FeSe}_{1.936}$ , and the third 1.0551 g of  $\text{FeSe}_{1.973} + 0.8002$  g elemental Se giving a gross composition  $\text{FeSe}_{4.005}$  in the sample container. The volume of the containers used was 25.4, 29.5, and 25.7  $\text{cm}^3$ , respectively, and the volume of the spiral-gauge + communication capillary was 2  $\text{cm}^3$ . The necessary corrections have been made in the calculations for those cases exhibiting a significant change in sample composition due to evaporation of selenium.

### Vapour pressure measurements with Knudsen cells

In the Knudsen effusion method a small proportion of the gas molecules in an equilibrium chamber passes through a small hole into a space of high vacuum. The number of molecules effusing per second through a hole of known area is related, by the kinetic theory of gases, to the interior partial pressure and the temperature and molecular weight of the gas. The following expression applies for the equilibrium pressure:

$$p_{i(\text{torr})} = 17.14 \frac{\Delta w_i}{atC} \left( \frac{T}{M_i} \right)^{\frac{1}{2}}$$

$\Delta w_i$  = weight loss (gram);  $a$  = area of effusion orifice ( $\text{cm}^2$ );  $t$  = time (seconds);  $C$  = Clausing factor (a correction factor<sup>16</sup> applied to the measured orifice area to determine the effective area);  $T$  = temperature (K);  $M_i$  = molecular weight of species  $i$  in the vapour.

Since the effusion method is a dynamic one small gaseous impurities have a negligible effect on the measured vapour pressures. The errors introduced in the measurements are thus related to the cell geometry (including the orifice) and to the technique used in establishing the weight loss.

Several authors<sup>16-19</sup> have discussed the problems arising from orifice non-ideality when employing effusion cells. To obtain significant vapour pressure information, data must be taken from cells having different orifice areas. These data can be converted to vapour pressure values taking into consideration the appropriate Clausing factors to determine the effective effusion area in each case.

In this study two cells were employed with effective effusion areas  $0.8415 \times 10^{-2} \text{ cm}^2$  (A) and  $0.6123 \times 10^{-2} \text{ cm}^2$  (B), respectively.

Preliminary tests with KCl gave third law values for standard heat of sublimation which are within  $\pm 2\%$  of literature values.<sup>31</sup>

### Selenium vapour

The selenium vapour consists of several molecular species. The following constants (standard state, ideal gas of 1 atm) for the equilibrium between the species were employed in the calculations:

1. $\text{Se} = 0.5 \text{ Se}_2$	$\log K = 7\,970/T + 0.1 \log T - 3.100$
2. $\text{Se}_3 = 1.5 \text{ Se}_2$	$\log K = -2\,812/T + 4.085$
3. $\text{Se}_6 = 2.5 \text{ Se}_2$	$\log K = -9\,880/T + 9.25$
4. $\text{Se}_6 = 3 \text{ Se}_3$	$\log K = -14\,200/T + 14.95$
5. $\text{Se}_7 = 3.5 \text{ Se}_2$	$\log K = -17\,080/T + 17.97$
6. $\text{Se}_8 = 4 \text{ Se}_2$	$\log K = -20\,130/T + 21.76$

The equilibrium constant for reaction 1 was calculated by means of  $D_0^\circ = 72.94 \pm 0.05 \text{ kcal}^{20}$  for the dissociation of  $\text{Se}_2$  and the heat capacities for the Se and  $\text{Se}_2$  molecules.<sup>21</sup> The constants for reactions 2–6 are taken from Berkowitz and Chupka.<sup>22</sup> In calculating the vapour pressure of pure liquid selenium, Brooks' <sup>23</sup> equation,  $\log p$  (torr) =  $-4989.5 \pm 4.5/T + 8.0886 \pm 0.0048$ , was employed.

The standard enthalpy of formation for  $\text{Se}_2(\text{g})$  is taken as  $33.3 \pm 0.5 \text{ kcal}$ , and the standard entropy as  $58.2 \pm 0.9 \text{ cal/deg mol}$  (Mills <sup>24</sup>). The splitting ( $1000 \pm 500 \text{ cm}^{-1}$ ) of the ground state for the  $\text{Se}_2$  molecule, which involves an electronic partition function contribution to the enthalpy and entropy, has been taken into consideration <sup>24</sup> in the thermochemical calculations.

## RESULTS AND DISCUSSION

### The pressure curves

In a binary system where one of the components is easily volatilized, the vapour pressures can be utilized in estimating several thermodynamic properties of the system. By employing the van't Hoff isobar:

$$\frac{d \ln p}{d(1/T)} = - \frac{\Delta H^\circ}{R}$$

a plot of the logarithm of the vapour pressures *versus* the reciprocal of the absolute temperature, forms a line where the slope gives the heat of reaction with the substances in their reference states, and the intersection of the line

with the  $1/T$  axis gives the entropy change. A straight line implies that the heat capacity of the gas and the condensed phases are the same, and that the composition of the substances does not change. If this condition is not met, the line will be curved. In a van't Hoff plot a phase change makes itself evident as a change of direction of the line; the way the direction changes depends on the reaction concerned.

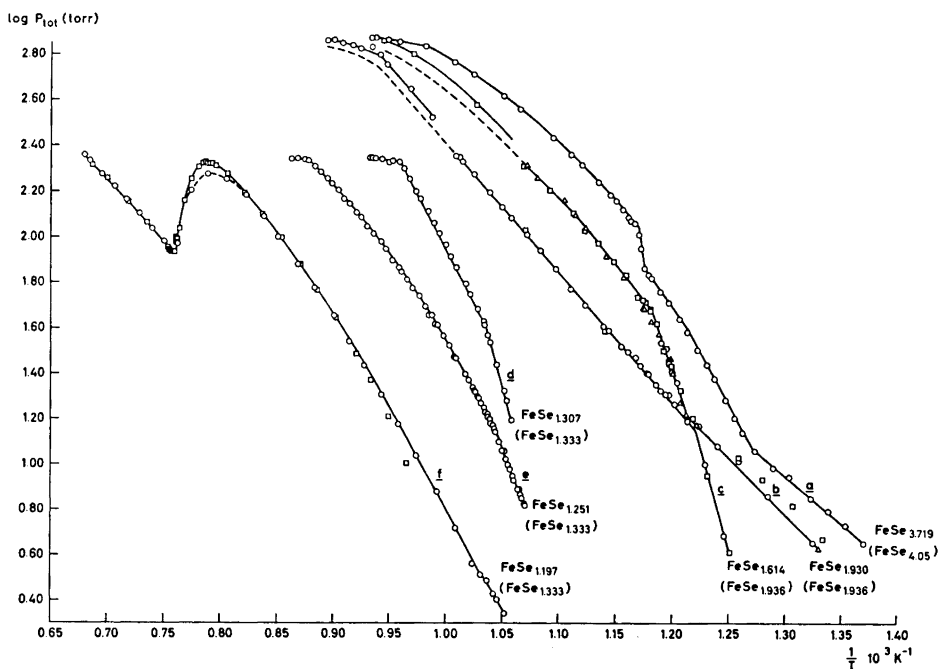


Fig. 2. van't Hoff plot with different selenium content. Pressures determined by silica manometer.

Fig. 2 shows some of the pressure curves obtained in experiments with decreasing selenium content. The starting compositions (in parentheses) and the actual ones are given. The figure shows one of the five curves, *a*, obtained in the composition range 80–66.6 at. % Se. The first linear part of the curve, starting at low temperature, shows the vapour pressures of molten selenium saturated with  $\text{FeSe}_2$ . These pressures are substantially lower than those for pure liquid selenium, being approximately one fifth of the values.

The partial molar heat of solution of liquid selenium in the  $\text{FeSe}_2$  saturated liquid is obtained by converting the pressures to activities in terms of the partial pressure of the  $\text{Se}_2$  gas molecule:

$$a_{\text{Se}} = (p_{\text{Se}_2}/p_{\text{Se}_2}^\circ)^{\frac{1}{2}}$$

and making a van't Hoff plot of  $R \ln a_{\text{Se}}$  versus  $1/T$ . In the expression for the activity,  $p_{\text{Se}_2}$  is the partial pressure over the alloy and  $p_{\text{Se}_2}^\circ$  is the partial pressure

Table 2. Partial molar heat of solution of liquid selenium in liquid selenium saturated with FeSe<sub>2</sub>.

Alloy	Temp. interval °C	Number of measurements	$\Delta\bar{H}_{\text{Se}}$ (kcal)
FeSe <sub>3.88</sub>	459–519	8	0.996
FeSe <sub>3.72</sub>	457–512	7	1.491
FeSe <sub>3.36</sub>	493–523	5	0.958
FeSe <sub>2.93</sub>	484–527	6	1.330
FeSe <sub>2.11</sub>	448–526	10	0.646
			Average 1.08 ± 0.33

over pure liquid selenium at the same temperature as the alloy. The least squares results for the plots are presented in Table 2.

Strictly, the equation used in deriving the partial molar heat of solution should only be applied to solutions of fixed composition, but the solubility of iron diselenide in selenium does not change significantly within the specified temperature interval. Dutrizac *et al.*<sup>12</sup> report a solubility of 40 ppm Fe at 585°C and 25 ppm Fe at 220°C. The low, positive heat effect found for the solution of selenium is consistent with the value found by Dutrizac for the partial molar heat of solution of iron in liquid selenium (+1 kcal).

Curve *a* in Fig. 2 shows two breaks. The first is a single, the second a double break. The double break is connected with the incongruent melting of FeSe<sub>2</sub>. The explanation of the first break is uncertain, but a lack of proper equilibrium in the sample might be the cause. The curves *b* and *c* show pressure data with FeSe<sub>1.936</sub> as starting material. In curve *b* the composition of the sample lies within the homogeneity range of FeSe<sub>2</sub>. Curve *c* shows the equilibrium between FeSe<sub>2</sub> and the NiAs-like phase below 550°C, and at higher temperature, after the break of the curve, the equilibrium between the NiAs-like phase and liquid selenium. Incidentally, this curve together with a second (not shown) indicate that the FeSe<sub>2</sub>-phase disappears at a lower temperature (550°C) than that found by means of DTA-analysis. The curves *d*, *e*, and *f* show pressure data with FeSe<sub>1.333</sub> as starting material. The break in curve *d* and *e* is connected with the transition from monoclinic to hexagonal NiAs-like phase. Curve *f* shows pressure data for a composition close to that of the congruently melting compound.

Fig. 3 shows isotherms at temperatures below and above 585°C, with composition range FeSe<sub>3.88</sub>–FeSe<sub>1.15</sub>. On the isotherm at 530°C, there are two horizontal parts, which demonstrate the equilibrium between liquid selenium and iron diselenide, at high selenium content, and the equilibrium between iron diselenide and the NiAs-like phase at low selenium content. On the isotherm at 640°C, the gaseous impurities make themselves so evident that a horizontal region hardly can be seen.

Although the incongruent melting of FeSe<sub>2</sub> has been observed by several investigators, the solid phase formed in the process has not been analysed. For this reason, the diselenide was quenched from 585°C, and the unknown

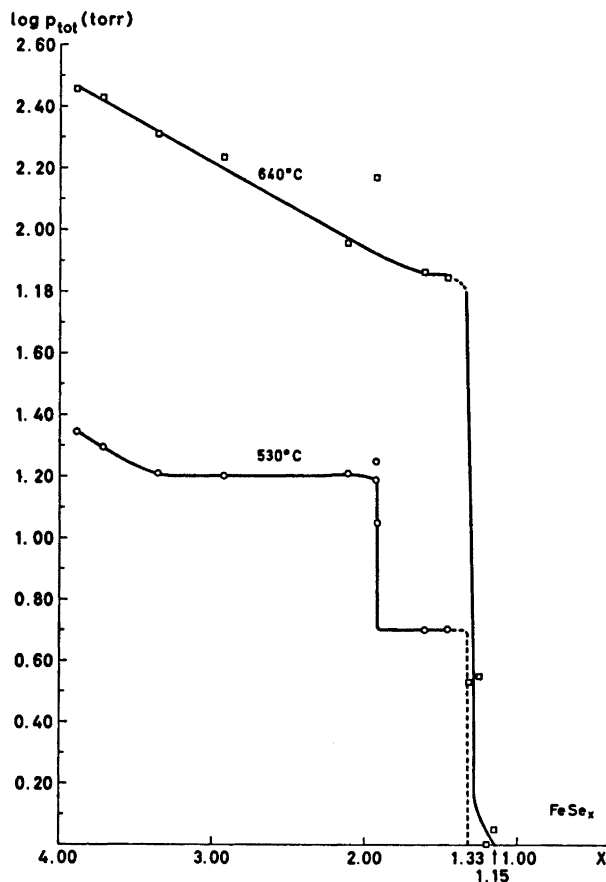
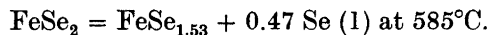


Fig. 3. Pressure isotherms as a function of selenium content.

phase analysed with a micro-probe. From two different parts of the specimen the solid was found to contain 60.5 and 60.7 at. % selenium, giving an average of 60.6 at. % selenium, *e.g.*  $\text{FeSe}_{1.53}$ . The equation for the incongruent melting of the diselenide can therefore be expressed:



The solid phase formed is the NiAs-like phase, which at this composition is very nearly hexagonal, judging from high temperature X-ray diagrams.

The selenium-poor phase limit of the hexagonal phase was determined at 804°C and 855°C by means of a Knudsen cell. The starting materials were  $\text{FeSe}_{1.143}$  and  $\text{FeSe}_{1.040}$ , respectively. Fig. 4 shows the partial molar free energy of solution of  $\text{Se}_2(\text{g})$  as a function of alloy composition. From the isotherms it can be seen that the hexagonal phase is stoichiometric at 804°C, but at 855°C the limit decreases to 49.34 at. % selenium. The Knudsen cell measurements



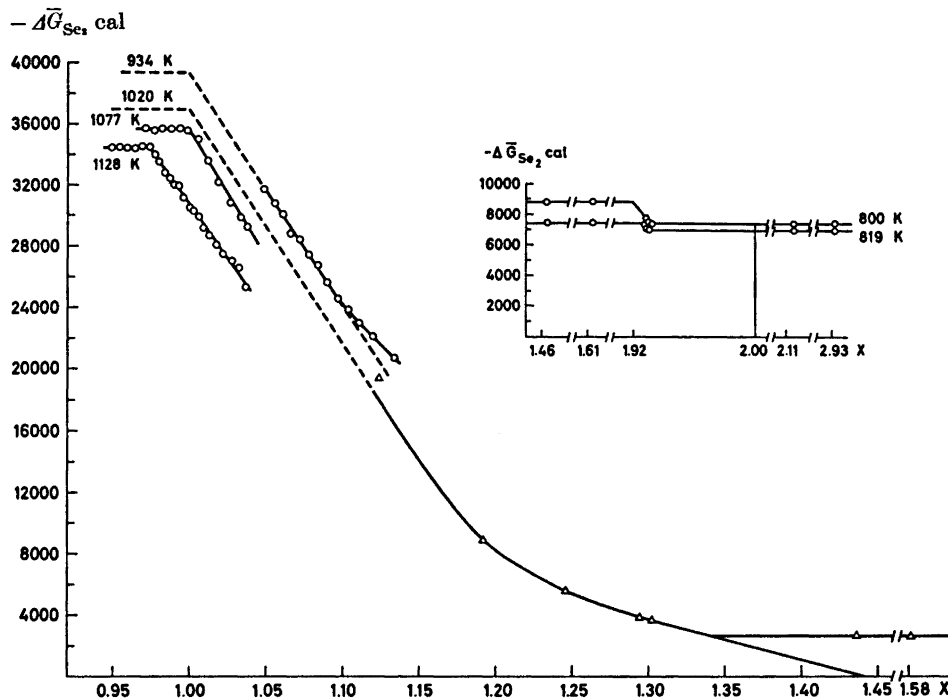


Fig. 4. Partial molar Gibbs energy of solution of  $\text{Se}_2(\text{g})$  as a function of selenium content.

were performed below  $872^\circ\text{C}$  because at this temperature a melt is formed as is evident through its strong attack on silica.

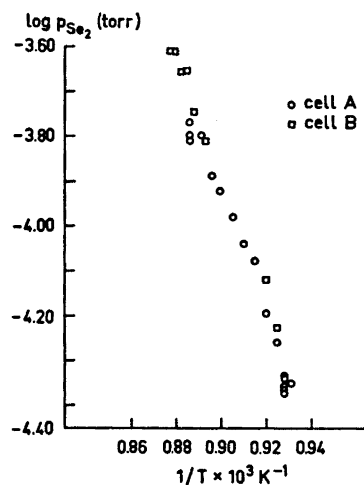


Fig. 5. van't Hoff plot of the hexagonal NiAs-like phase in equilibrium with iron. Pressures determined by Knudsen cells.

Since the hexagonal phase limit is stoichiometric at 804°C it is probable that this is so also at lower temperatures when the hexagonal phase is formed from the tetragonal phase by the peritectoid reaction:

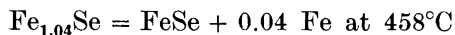


Fig. 5 shows a plot of the logarithm of the partial pressure of  $\text{Se}_2(\text{g})$  of the hexagonal phase in equilibrium with iron as a function of temperature.

#### T h e r m o c h e m i c a l c a l c u l a t i o n s

In calculating the standard enthalpy of formation both the second- and third-law method were employed. Third-law values were calculated by the equation:

$$\Delta H_{298 \text{ reac}} = \Delta G_{T \text{ reac}}^\circ - T \Delta \text{fef}_{\text{reac}}$$

$\Delta \text{fef}$  is the change in the free-energy functions:

$$\text{fef} = (H_T - H_{298}^\circ)/T - S_T^\circ$$

for the different species taking part in the reactions.

Gibbs free energy of reaction in the homogeneity ranges was found by graphical integration of Gibbs-Duhem equation:

$$\Delta G_{\text{reac}} = N_{\text{Fe}} \int_0^x \Delta \bar{G}_{\text{Se}_2} dx$$

where  $\Delta \bar{G}_{\text{Se}_2}$  is the partial molar free energy of solution of  $\text{Se}_2(\text{g})$  molecule, and  $x = N_{\text{Se}}/N_{\text{Fe}}$  is the ratio between the atomic fractions for selenium and iron.

In the second-law method the forms of the Gibbs-Duhem equations are:

$$\Delta H_{\text{reac}} = N_{\text{Fe}} \int_0^x \Delta \bar{H}_{\text{Se}_2} dx, \quad \text{and}$$

$$\Delta S_{\text{reac}} = N_{\text{Fe}} \int_0^x \Delta \bar{S}_{\text{Se}_2} dx$$

where  $\Delta \bar{H}_{\text{Se}_2}$  and  $\Delta \bar{S}_{\text{Se}_2}$  are the partial molar enthalpy and entropy of solution of gaseous  $\text{Se}_2$ , respectively.

Tables 3–5 contain all the data employed in the subsequent calculations. *FeSe*. The solubility of selenium in iron is less than 0.5 at. % at 1200 K,<sup>10</sup> and the integral Gibbs energy of reaction is thus practically equal to zero. In the two-phase region FeSe is therefore considered to be in equilibrium with pure iron. Table 6 presents the standard enthalpy of formation for FeSe based on third-law values. Only pressures near 1077 K are used in the calculations, where the stoichiometric reaction  $2\text{Fe} + \text{Se}_2(\text{g}) = 2\text{FeSe}$  applies. The enthalpy and entropy values for FeSe as a function of temperature are interpolated from data for  $\text{FeSe}_{0.96}$  and  $\text{FeSe}_{1.143}$ <sup>13</sup> and extrapolated above 1050K which

Table 3. Pressure data from Knudsen cells.

Fe + FeSe region	Temp. K	Time, sec	Weight loss, mg	Partial pressure $p_{\text{Se}_2}$ , atm	$-\Delta\bar{G}_{\text{Se}_2}$ , cal
Cell					
A	1074	246 600	2.206	$5.845 \times 10^{-8}$	35 546
A	1081	172 800	1.893	$7.178 \times 10^{-8}$	35 329
A	1087	169 800	2.177	$8.416 \times 10^{-8}$	35 188
A	1092	166 200	2.770	$1.101 \times 10^{-7}$	34 768
A	1099	152 700	2.812	$1.216 \times 10^{-7}$	34 774
A	1105	167 700	3.493	$1.376 \times 10^{-7}$	34 692
A	1111	163 800	3.900	$1.574 \times 10^{-7}$	34 602
A	1116	154 800	4.244	$1.817 \times 10^{-7}$	34 420
A	1121	169 800	5.326	$2.082 \times 10^{-7}$	34 289
B	1126	86 400	2.244	$2.374 \times 10^{-7}$	34 124
B	1140	85 500	2.996	$3.212 \times 10^{-7}$	33 873
B	1137	89 400	3.145	$3.230 \times 10^{-7}$	33 777
B	1134	86 700	2.742	$2.899 \times 10^{-7}$	33 914
B	1130	79 920	2.539	$2.918 \times 10^{-7}$	33 791
B	1119	81 900	1.826	$2.035 \times 10^{-7}$	34 264
B	1081	162 000	1.333	$7.417 \times 10^{-8}$	35 263
B	1087	241 200	2.657	$9.993 \times 10^{-8}$	34 805
Cell A, FeSe <sub>x</sub>					
x: 1.134	934	1 800	3.873	$1.401 \times 10^{-5}$	20 742
1.120	»	2 460	2.498	$6.612 \times 10^{-6}$	22 136
1.111	»	3 000	1.897	$4.117 \times 10^{-6}$	23 015
1.104	»	5 100	2.045	$2.611 \times 10^{-6}$	23 861
1.097	»	7 200	1.950	$1.763 \times 10^{-6}$	24 589
1.090	»	11 160	1.685	$9.825 \times 10^{-7}$	25 674
1.084	»	18 000	1.515	$5.475 \times 10^{-7}$	26 760
1.078	»	26 100	1.505	$3.749 \times 10^{-7}$	27 462
1.072	»	39 780	1.350	$2.205 \times 10^{-7}$	28 448
1.066	»	68 400	1.860	$1.766 \times 10^{-7}$	28 859
1.061	»	87 300	1.196	$8.888 \times 10^{-8}$	30 134
1.056	»	162 900	1.522	$6.056 \times 10^{-8}$	30 846
1.049	»	345 600	1.982	$3.712 \times 10^{-8}$	31 755
1.038	1077	3 600	0.596	$1.140 \times 10^{-6}$	29 288
1.034	»	14 400	1.774	$8.459 \times 10^{-7}$	29 926
1.027	»	25 200	2.030	$5.506 \times 10^{-7}$	30 845
1.019	»	44 100	1.913	$2.940 \times 10^{-7}$	32 188
1.012	»	73 800	1.660	$1.506 \times 10^{-7}$	33 620
1.006	»	155 400	1.833	$7.763 \times 10^{-8}$	35 038
0.999	»	173 100	1.605	$6.055 \times 10^{-8}$	35 569
0.994	»	172 500	1.469	$5.544 \times 10^{-8}$	35 758
0.988	»	174 900	1.533	$5.712 \times 10^{-8}$	35 694
0.982	»	165 600	1.406	$5.527 \times 10^{-8}$	35 765
0.977	»	172 800	1.585	$5.987 \times 10^{-8}$	35 593
0.971	»	173 700	1.479	$5.543 \times 10^{-8}$	35 758
1.037	1128	1 920	3.343	$1.233 \times 10^{-5}$	25 336
1.032	»	2 100	2.080	$6.993 \times 10^{-6}$	26 608
1.028	»	3 600	2.897	$5.672 \times 10^{-6}$	27 077
1.022	»	4 800	3.161	$4.634 \times 10^{-6}$	27 530
1.017	»	4 920	2.520	$3.596 \times 10^{-6}$	28 099
1.013	»	5 400	2.075	$2.690 \times 10^{-6}$	28 750
1.009	»	7 200	2.271	$2.203 \times 10^{-6}$	29 198

Table 3. Continued.

1.006	1128	7 200	1.645	$1.588 \times 10^{-6}$	29 931
1.003	»	9 000	1.687	$1.299 \times 10^{-6}$	30 381
0.999	»	10 800	1.893	$1.213 \times 10^{-6}$	30 534
0.996	»	14 580	1.904	$8.993 \times 10^{-7}$	31 206
0.993	»	11 700	1.084	$6.333 \times 10^{-7}$	31 992
0.991	»	20 220	1.822	$6.156 \times 10^{-7}$	32 055
0.987	»	25 200	1.881	$5.076 \times 10^{-7}$	32 488
0.984	»	30 600	1.948	$4.310 \times 10^{-7}$	32 854
0.981	»	36 000	1.682	$3.134 \times 10^{-7}$	33 569
0.977	»	43 200	1.633	$2.517 \times 10^{-7}$	34 060
0.974	»	77 880	2.438	$2.069 \times 10^{-7}$	34 499
0.969	»	86 400	2.620	$2.002 \times 10^{-7}$	34 573
0.964	»	86 400	2.785	$2.133 \times 10^{-7}$	34 431
0.959	»	86 400	2.872	$2.203 \times 10^{-7}$	34 359
0.954	»	87 900	2.756	$2.073 \times 10^{-7}$	34 495
0.949	»	87 900	2.833	$2.133 \times 10^{-7}$	34 431
Cell B					
1.124	1020	1 200	8.890	$6.924 \times 10^{-5}$	19 413

Table 4. Measurements with silica manometer.

Composition at room temp.	Composition	Total pressure torr	Partial press. Se <sub>2</sub> , torr	$-\Delta\bar{G}_{\text{Se}_2}$ , cal
	at 1020 K			
FeSe <sub>1.197</sub>	FeSe <sub>1.192</sub>	9.77	9.68	8844
FeSe <sub>1.251</sub>	FeSe <sub>1.246</sub>	52.00	49.18	5549
FeSe <sub>1.307</sub>	FeSe <sub>1.294</sub>	138.0	116.4	3802
FeSe <sub>1.316</sub>	FeSe <sub>1.302</sub>	150.0	124.6	3664
FeSe <sub>1.464</sub>	FeSe <sub>1.436</sub>	288.0	203.8	2667
FeSe <sub>1.614</sub>	FeSe <sub>1.531</sub>	335.0	226.2	2455
	at 819 K			
FeSe <sub>1.464</sub>	FeSe <sub>1.464</sub>	13.18	7.67	7478
FeSe <sub>1.614</sub>	FeSe <sub>1.614</sub>	14.13	8.01	7409
	at 800 K			
FeSe <sub>1.464</sub>	FeSe <sub>1.464</sub>	3.84	2.90	8851
FeSe <sub>1.614</sub>	FeSe <sub>1.614</sub>	4.02	3.00	8798
	at 819 K			
FeSe <sub>1.930</sub>	FeSe <sub>1.927</sub>	14.96	8.29	7353
FeSe <sub>1.932</sub>	FeSe <sub>1.929</sub>	19.82	9.76	7086
FeSe <sub>1.934</sub>	FeSe <sub>1.931</sub>	21.88	10.32	6996
	at 800 K			
FeSe <sub>1.930</sub>	FeSe <sub>1.929</sub>	10.64	5.66	7789
FeSe <sub>1.932</sub>	FeSe <sub>1.930</sub>	14.45	6.73	7512
FeSe <sub>1.934</sub>	FeSe <sub>1.933</sub>	16.98	7.35	7373
	at 819 K			
FeSe <sub>2.115</sub>	FeSe <sub>2.115</sub>	21.63	10.21	7010
FeSe <sub>2.932</sub>	FeSe <sub>2.932</sub>	22.13	10.34	6990
	at 800 K			
FeSe <sub>2.115</sub>	FeSe <sub>2.115</sub>	15.49	6.91	7460
FeSe <sub>2.932</sub>	FeSe <sub>2.932</sub>	14.79	6.74	7500

Table 5. Data for second-law treatment.

Composition at room temp.	Composition	$-\Delta\bar{H}_{\text{Se}_2}$ , cal	$-\Delta\bar{S}_{\text{Se}_2}$ , cal/deg
	at 1020 K		
Fe-FeSe	-	62 660	25.43
FeSe <sub>1.01</sub>	FeSe <sub>1.01</sub>	49 180	15.52
FeSe <sub>1.153</sub>	FeSe <sub>1.153</sub>	43 530	34.82
FeSe <sub>1.188</sub>	FeSe <sub>1.188</sub>	36 440	30.33
FeSe <sub>1.197</sub>	FeSe <sub>1.192</sub>	42 100	32.57
FeSe <sub>1.251</sub>	FeSe <sub>1.246</sub>	40 110	33.86
FeSe <sub>1.287</sub>	FeSe <sub>1.280</sub>	36 250	32.47
FeSe <sub>1.307</sub>	FeSe <sub>1.294</sub>	39 530	35.05
FeSe <sub>1.316</sub>	FeSe <sub>1.302</sub>	39 950	35.56
FeSe <sub>1.464</sub>	FeSe <sub>1.436</sub>	27 340	24.39
FeSe <sub>1.614</sub>	FeSe <sub>1.581</sub>	26 210	23.08
	at 800 K		
FeSe <sub>1.464</sub>	FeSe <sub>1.464</sub>	62 780	67.54
FeSe <sub>1.614</sub>	FeSe <sub>1.614</sub>	63 550	68.54
FeSe <sub>1.930</sub>	FeSe <sub>1.929</sub>	26 020	22.80
FeSe <sub>2.115</sub>	FeSe <sub>2.115</sub>	25 210	22.18

Table 6. Standard enthalpy of formation for FeSe.

Cell	<i>T</i> K	Time, sec	Weight loss, mg	Pressure <i>p</i> <sub>Se<sub>2</sub></sub> , atm	<i>d</i> f <sub>reac</sub> , cal/deg	$\Delta H^\circ_{298}$ , kcal/mol
A	1074	246 600	2.206	$5.845 \times 10^{-8}$	30.78	$-17.650 \pm 1.4$
A	1077	173 700	1.479	$5.543 \times 10^{-8}$	30.78	$-17.757 \pm 1.4$
A	1077	172 800	1.585	$5.987 \times 10^{-8}$	30.78	$-17.675 \pm 1.4$
A	1077	165 600	1.406	$5.527 \times 10^{-8}$	30.78	$-17.760 \pm 1.4$
A	1077	174 900	1.533	$5.712 \times 10^{-8}$	30.78	$-17.725 \pm 1.4$
A	1077	172 500	1.469	$5.544 \times 10^{-8}$	30.78	$-17.757 \pm 1.4$
A	1077	173 100	1.605	$6.055 \times 10^{-8}$	30.78	$-17.663 \pm 1.4$
A	1081	172 800	1.893	$7.178 \times 10^{-8}$	30.77	$-17.645 \pm 1.4$
B	1081	162 000	1.333	$7.417 \times 10^{-8}$	30.77	$-17.612 \pm 1.4$
B	1086	241 200	2.657	$9.993 \times 10^{-8}$	30.75	$-17.450 \pm 1.4$
A	1087	169 800	2.177	$8.416 \times 10^{-8}$	30.74	$-17.651 \pm 1.4$
					Average	$-17.667 \pm 1.4$

is the limit for the data cited. The sublimation of iron as FeSe molecules was found to be negligible compared to selenium, and the weight-losses are taken as being due to selenium only. An average of  $-17.7 \pm 1.4$  kcal/mol is found for the standard enthalpy of formation for FeSe at 298 K.

The standard error of  $\pm 1.4$  kcal/mol in the enthalpy of formation is based on the following estimates: the pressure variation is estimated to  $\pm 50\%$ , which gives an uncertainty of  $\pm 1.7$  kcal in  $\Delta G^\circ_{\text{reac}}$ . The uncertainty in the free-energy function for each substance taking part in the reaction is estimated

to  $\pm 0.25$  cal/deg for Fe and FeSe, and  $\pm 1.1$  cal/deg for  $\text{Se}_2$ . This gives an uncertainty of  $\pm 2.1$  cal/deg in  $\Delta f_{\text{react}}$  and  $\pm 2.25$  kcal in  $T \Delta f_{\text{react}}$ . The uncertainty in  $\Delta H_{298 \text{ K}}^\circ$  for  $\text{Se}_2$  is  $\pm 0.5$  kcal.

By integrating in the two-phase field up to  $x=0.96$  at high temperature the standard enthalpy of formation for  $\text{FeSe}_{0.96}$  is obtained:  $\Delta H_{298 \text{ K}}^\circ = -17.3 \pm 1.4$  kcal/mol.

*FeSe<sub>1.143</sub>* The standard enthalpy of formation for  $\text{FeSe}_{1.143}$  was derived by graphical integration with the reference temperature 934 K. At this temperature the pressures could not be measured below 51.21 at. % selenium ( $\text{FeSe}_{1.05}$ ) and an extrapolation down to FeSe was necessary. The reactions:



give the net reaction:

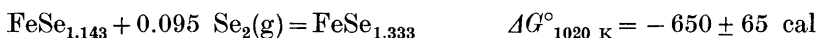


The change in the free-energy function for the net reaction is  $16.85 \pm 1.13$  cal/deg. Together with the standard enthalpy of formation for  $\text{Se}_2(\text{g})$  this gives a standard enthalpy of formation for  $\text{FeSe}_{1.143}$  of  $-18.3 \pm 1.5$  kcal/mol at 298 K.

*FeSe<sub>1.333</sub>*. The standard enthalpy of formation for  $\text{FeSe}_{1.333}$  was calculated with the reference temperature 1020 K. From enthalpy and entropy of reaction, the change in Gibbs energy for the following reaction is found:



From graphical integration one obtains:



The net reaction is:



The derived change in the free-energy function for the net reaction is  $21.22 \pm 1.23$  cal/deg at 1020 K. Together with the standard enthalpy of formation for  $\text{Se}_2(\text{g})$  this gives a standard enthalpy of formation of  $-20.5 \pm 2.1$  kcal/mol at 298 K for  $\text{FeSe}_{1.333}$ .

From the isotherm at 1020 K (Fig. 4), the selenium-rich limit of the NiAs-like phase is found to be at 57.3 at. % selenium ( $\text{FeSe}_{1.343}$ ). This value is not far from the composition of the solid phase formed at the monotectic at 793°C (1066 K). The solid phase quenched from this temperature contained an average of 57.4 at. % selenium ( $\text{FeSe}_{1.35}$ ). This result was found by microprobe analysis.

By means of the isotherm at 1020 K, Gibbs free energy of forming equilibrium mixtures of Fe and Se from solid iron and diatomic selenium gas at 1 atm is presented in Fig. 6. The minimum is at  $\text{FeSe}_{1.125}$  (52.94 at. % selenium) which is close to the composition that melts congruently.

*FeSe<sub>2</sub>*. From the isotherm plots it is seen that the selenium-poor limit of the diselenide is at  $\text{FeSe}_{1.920}$  at 800 K and at  $\text{FeSe}_{1.927}$  at 819 K (Fig. 4). The

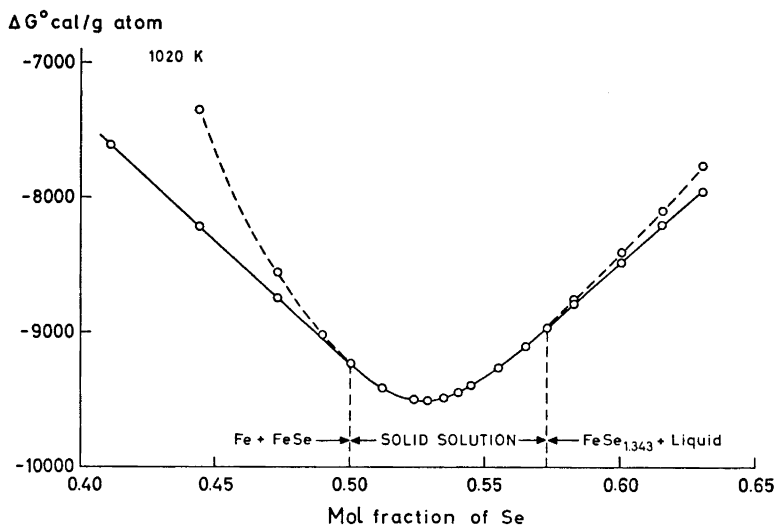


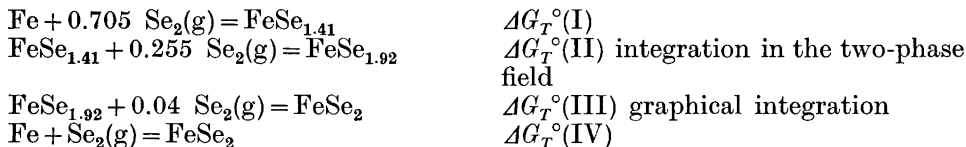
Fig. 6. The change in Gibbs free energy in forming mixtures of Fe and Se from solid iron and diatomic selenium gas at 1 atm.

extrapolations made in the plots are believed to be correct to  $\pm 0.005$  units in the atomic fraction ratio.

In the same temperature interval, high temperature X-ray photographs show that the selenium-rich limit of the NiAs-like phase expands from 58.5 to 59.0 at. % selenium ( $\text{FeSe}_{1.41}$ – $\text{FeSe}_{1.44}$ ).

The free-energy function for  $\text{FeSe}_2$  in the above mentioned temperature interval is:  $\text{fef}_{800\text{ K}} = -27.63 \pm 0.39$  cal/deg,  $\text{fef}_{819\text{ K}} = -27.97 \pm 0.40$  cal/deg, and the enthalpy change:  $H_{800} - H_{298\text{ K}} = 11\,316 \pm 180$  cal,  $H_{819} - H_{298\text{ K}} = 12\,178 \pm 190$  cal. These values are taken from recent measurements<sup>25</sup> using a drop calorimeter.

The standard enthalpy of formation for  $\text{FeSe}_{1.41}$ – $\text{FeSe}_{1.44}$  was found by extrapolation from the 1020 K isotherm. Table 7 presents the standard enthalpy of formation of  $\text{FeSe}_2$ , which in average is  $-29.4 \pm 2.9$  kcal/mol at 298 K. The Roman numbers in the table refer to the following type of reactions:



In the second-law treatment the integration was carried out with the reference temperature 1020 K up to  $\text{FeSe}_{1.41}$ . From this composition the integration up to  $\text{FeSe}_2$  was continued with the reference temperature 800 K. Table 8 presents both the second- and third-law values found. Also shown are

Table 7. Standard enthalpy of formation of FeSe<sub>2</sub>.

Over-all comp.	T K	Comp. of the NiAs-like phase	Comp. of FeSe <sub>2</sub>	$p_{\text{Se}_2}$ (torr)	$p_{\text{Se}_2}$ (atm)	$\Delta G_{\text{Se}_2}$ (kcal)	$\Delta H_{\text{f,298}}^{\circ}$ NiAs-like phase kcal	$\Delta G_{\text{f}}^{\circ}$ (I) kcal	$\Delta G_{\text{f}}^{\circ}$ (II) kcal	$\Delta G_{\text{f}}^{\circ}$ (III) kcal	$\Delta G_{\text{f}}^{\circ}$ (IV) kcal	$\Delta f_{\text{f}}^{\circ}$ (V) cal/deg	$\Delta H_{\text{f,298}}^{\circ}$ FeSe <sub>2</sub> kcal/mol
FeSe <sub>1.614</sub>	798.9	FeSe <sub>1.41</sub>	FeSe <sub>1.920</sub>	4.08	3.00	-8.78	-21.26	-25.72	-2.24	-0.31	-28.27	43.09	-29.40 ± 2.86
»	802.1	»	»	4.83	3.46	-8.59	-21.26	-25.59	-2.19	-0.31	-28.09	43.07	-29.34 ± 2.86
»	811.9	FeSe <sub>1.43</sub>	FeSe <sub>1.924</sub>	8.88	5.63	-7.91	-21.34	-25.52	-1.95	-0.30	-27.77	43.02	-29.40 ± 2.86
»	813.6	»	»	10.06	9.19	-7.77	-21.34	-25.44	-1.92	-0.30	-27.60	43.02	-29.36 ± 2.86
FeSe <sub>1.464</sub>	803.1	FeSe <sub>1.41</sub>	FeSe <sub>1.920</sub>	5.08	3.62	-8.53	-21.26	-25.59	-2.17	-0.31	-28.07	43.08	-29.37 ± 2.86
»	813.6	FeSe <sub>1.43</sub>	FeSe <sub>1.924</sub>	9.42	5.94	-7.84	-21.34	-25.44	-1.93	-0.30	-27.67	43.02	-29.37 ± 2.86
»	818.6	FeSe <sub>1.44</sub>	FeSe <sub>1.927</sub>	13.17	7.65	-7.48	-21.45	-25.35	-1.82	-0.28	-27.44	42.99	-29.34 ± 2.86
													Average 29.37 ± 2.86

Table 8. Present and previously reported thermodynamic data for the iron selenides.

Vapour pressure, this work		Calorimetry		Calorimetry heat of synthesis		Solution calorimetry		Vapour pressure	
Third-law	Second-law	Grønqvold <sup>13,30</sup>	Kapushinskii and Golutvin <sup>26</sup>	Rossini et al. <sup>27</sup>	Azerbaeva and Tseft <sup>28</sup>	Rumyantsev et al. <sup>29</sup>			
$\Delta H_{\text{f,298}}^{\circ}$ kcal mol <sup>-1</sup>	$\Delta H_{\text{f,298}}^{\circ}$ kcal mol <sup>-1</sup>	$\Delta H_{\text{f,298}}^{\circ}$ kcal mol <sup>-1</sup>	$\Delta H_{\text{f,298}}^{\circ}$ kcal mol <sup>-1</sup>	$\Delta H_{\text{f,298}}^{\circ}$ kcal mol <sup>-1</sup>	$\Delta H_{\text{f,298}}^{\circ}$ kcal mol <sup>-1</sup>	$\Delta H_{\text{f,298}}^{\circ}$ kcal mol <sup>-1</sup>	$\Delta H_{\text{f,298}}^{\circ}$ kcal mol <sup>-1</sup>	$S_{\text{298}}^{\circ}$ cal deg <sup>-1</sup> mol <sup>-1</sup>	$\Delta H_{\text{f,298}}^{\circ}$ kcal mol <sup>-1</sup>
FeSe <sub>0.96</sub>	-17.3 ± 1.4	-17.5 ± 2.3	16.72 ± 1.11	16.88					
FeSe	-17.7 ± 1.4	-17.7 ± 2.3	17.65 ± 1.11	(17.77)					
FeSe <sub>1.143</sub>	-18.3 ± 1.5	-17.5 ± 2.5	21.50 ± 1.17	20.96					
FeSe <sub>1.333</sub>	-20.5 ± 2.1	-19.1 ± 2.6	23.31 ± 1.30	22.29					
FeSe <sub>2</sub>	-29.4 ± 2.9	-28.2 ± 3.2	21.49 ± 1.93	20.76	-16.5	-13.9	17.27		-11.7

Note added in proof. F. Grønqvold has published his work on enthalpy of formation of FeSe<sub>0.96</sub>, FeSe<sub>1.143</sub> and FeSe<sub>1.333</sub> by means of a high-temperature reaction calorimeter (*Acta Chem. Scand.* **26** (1972) 2086). His values for standard enthalpy of formation at 298 K for the compositions mentioned are: -16.0 kcal/mol, -15.8 kcal/mol and 16.9 kcal/mol, respectively. The numerical values, especially the two last mentioned, seem to be too low. The calculation of the standard free energy of formation of FeSe<sub>2</sub> at 298 K by combining the decomposition pressure of this compound with the appropriate thermodynamic data deduced from Grønqvold's values, indicates that the NiAs-like phases should be unstable at this temperature.



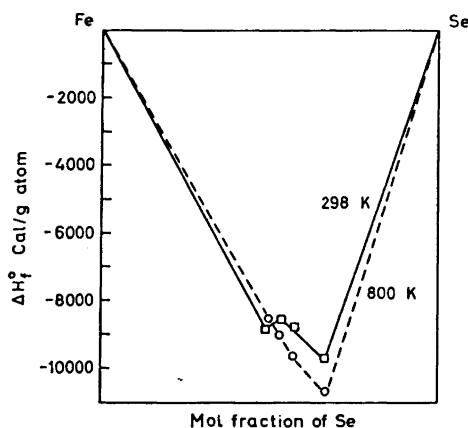


Fig. 7. Standard enthalpy of formation per gram atom alloy based on third-law values.

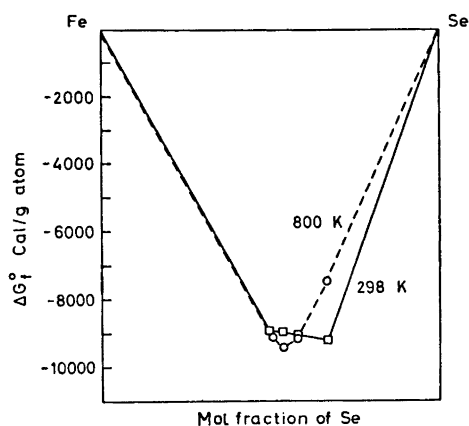


Fig. 8. Standard Gibbs free energy of formation per gram atom alloy based on third-law values.

the results of other workers.<sup>26-29</sup> The entropy of  $\text{FeSe}_{0.96}$  due to Grønvold<sup>13</sup> has been corrected for structural zero-point entropy.

When the second- and third-law enthalpy of formation values are compared, a reasonable agreement is found within the limits of error. The agreement is better for the two first than for the three last compositions. If the entropies for  $\text{FeSe}_{1.143}$  and  $\text{FeSe}_{1.333}$  should be higher, the divergence would be less. Earlier investigators<sup>7</sup> were not certain that complete magnetic and structural order in the two compositions had been attained in the region 0–5 K.

Figs. 7 and 8 show standard enthalpy and Gibbs free energy of formation per gram atom alloy based on the third-law values at 298 K and 800 K. The selenium-poorest composition is  $\text{Fe}_{0.510}\text{Se}_{0.490}$  at 298 K and  $\text{Fe}_{0.500}\text{Se}_{0.500}$  at 800 K. At 800 K the standard state for selenium is the liquid. The standard enthalpy of formation has its lowest value corresponding to the diselenide both at high and low temperatures, giving an irregular shape to the curve at 298 K. The standard Gibbs energy of formation has its minimum near  $\text{FeSe}_{1.145}$  at 800 K, but at 298 K this has moved to  $\text{FeSe}_2$ . At this temperature the standard entropy of formation of this compound is less negative and the  $-T\Delta S$  term makes a smaller reduction of the large negative standard enthalpy of formation value.

#### REFERENCES

1. Hägg, G. and Kindström, A. L. *Z. Phys. Chem.* **21** (1933) 453.
2. Tengner, S. *Z. anorg. allgem. Chem.* **239** (1938) 126.
3. Haraldsen, H. and Grønvold, F. *Tidskr. Kjemi Bergvesen Met.* **10** (1944) 98.
4. Hirone, T., Maeda, S. and Tsuga, N. *J. Phys. Soc. Japan* **9** (1954) 496.
5. Hirone, T. and Chiba, S. *J. Phys. Soc. Japan* **17** (1956) 666.
6. Okazaki, I. A. and Hirakawa, K. *J. Phys. Soc. Japan* **11** (1956) 930.
7. Grønvold, F. and Westrum, E. *Acta Chem. Scand.* **13** (1959) 241.

8. Okazaki, A. *J. Phys. Soc. Japan* **16** (1961) 1162.
9. Trøften, P. and Kullerud, G. *Carnegie Inst. Wash. Papers Geophys. Lab. No. 1363* (1961) 176.
10. Kullerud, G. *Carnegie Inst. Wash. Year Book* **67** (1967–1968) 175.
11. Dutrizac, J. E., Janjua, M. and Toguri, J. *Can. J. Chem.* **46** (1968) 1171.
12. Dutrizac, J. E., Janjua, M. and Toguri, J. *Can. Met. Quart.* **7** (1968) 91.
13. Grønvold, F. *Acta Chem. Scand.* **22** (1968) 1219.
14. Haraldsen, H., Kjekshus, A., Røst, E. and Steffensen, A. *Acta Chem. Scand.* **17** (1963) 1283.
15. Andresen, A. F. and Svendsen, S. R. *Unpublished results.*
16. Schulz, D. A. and Searcy, A. W. *J. Chem. Phys.* **36** (1962) 3099.
17. Rossman, M. S. and Yarwood, J. *J. Chem. Phys.* **21** (1953) 1406.
18. Speiser, R. and Johnston, H. L. *Trans. Am. Soc. Metals* **42** (1950) 283.
19. Whitman, C. I. *J. Chem. Phys.* **20** (1952) 161.
20. Barrow, R. F., Chandler, G. G. and Meyer, C. B. *Phil. Trans. Roy. Soc. (London), Ser. A* **260** (1966) 395.
21. Kelley, K. K. *U. S. Bur. Mines Bull.* **584** (1960).
22. Berkowitz, Y. and Chupka, W. A. *J. Chem. Phys.* **45** (1966) 4289.
23. Brooks, L. S. *J. Am. Chem. Soc.* **74** (1952) 227.
24. Mills, K. C. National Physical Laboratory, Teddington, England. *Personal communication.*
25. Svendsen, S. R. *To be published.*
26. Kapusinskii, A. F. and Golutvin, U. M. *Zh. Fiz. Khim.* **25** (1951) 729.
27. Rossini, F. D., Wagnan, D. D., Evans, W. H., Levine, S. and Jaffe, I. *Natl. Bur. Std. (U.S.) Circ.* **500** (1952).
28. Azerbaeva, R. G. and Tseft, A. L. *Tr. Inst. Met. Obogashch. Akad. Nauk. Kaz. SSR* **8** (1963) 50.
29. Ruamyantsev, Y. M., Zhitenva, G. M. and Bolandz, F. M. *Tr. Vost Sib. Filiala, Akad. Nauk. SSSR* **41** (1962) 114.
30. Grønvold, F. and Westrum, E. F. *Inorg. Chem.* **1** (1962) 36.
31. Hill, S. D., Adams, H. and Block, F. E. *U.S. Bur. Mines, Rep. Invest.* (1966), No. 6849.

Received February 16, 1972.